NEW ROTOR TEST RIG IN THE LARGE MODANE WIND TUNNEL

M. ALLONGUE - AEROSPATIALE - HELICOPTERS DIVISION - Marignane - FRANCE

J. P. DREVET - ONERA - GRANDS MOYENS D'ESSAIS -Modane - FRANCE

FIFTEENTH EUROPEAN ROTORCRAFT FORUM

SEPTEMBER 12 - 15, 1989 AMSTERDAM

NEW ROTOR TEST RIG IN THE LARGE MODANE WIND TUNNEL

M. ALLONGUE (AEROSPATIALE - Helicopters Division)

J.P. DREVET (ONERA/GME)

ABSTRACT

From now on, helicopter rotor tests in the large S1MA wind tunnel at the Modane-Avrieux Center of ONERA will be conducted with a new "BERH" helicopter rotor test rig. The qualification tests were run in November 1987 and the first industrial test campaign - the tenth in S1MA - was conducted in August 1988. This document presents the possibilities of this new device and some results obtained during the tenth test campaign. The new bench is technically different from the previous one as concerns its support structure, drive system and instrumentation. These modifications have improved test productivity and measurement accuracy. With this new system, five rotors were tested in less than three weeks. The test method was thoroughly changed to include two major advantages. First, it avoids having to interpolate several times when comparing rotors. Secondly, we can compare the blade stresses on two rotors at the same lift and propulsive force. To allow this approach, a control aid program operates on line during the tests. During the tenth campaign, a large amount of data was generated, and the quality of the data was shown to be satisfactory.

NOTATION

a : Speed of sound, m/s

b : Number of blades

c : Airfoil chord, m

C_ℓ : Rotor lift coefficient = $L/[\rho\pi R^2(\Omega R)^2]$

C_D : Rotor drag coefficient = $D/[\rho\pi R^2(\Omega R)^2]$

C_Q : Rotor torque coefficient = $Q/[\rho\pi R^2(\Omega R)^2 R]$

D : Rotor drag, N

L : Rotor lift, N

M : Mach number=V/a

M_{tip}: Hover tip Mach number=$\Omega R/a$

Q : Rotor shaft torque, Nm

R : Rotor radius, m

r : Spanwise station, m

V : Free stream velocity, m/s

$\overline{X}$:Non-dimensional rotor propulsive force

$\overline{X}=D/[4\rho V^2\sigma R^2]$

α_S : Rotor shaft angle, deg

β : blade flapping angle, deg

$\beta(\psi)=\beta_0+\beta_{1C}\cos(\psi)+\beta_{1S}\sin(\psi)+\cdots$

μ : Rotor advance ratio=$V/(\Omega R)$

Ω : Rotor angular velocity, rad/s

ψ : Rotor blade azimuth angle,deg

ρ : Air density, Kg/m^3

σ : Rotor solidity=$bc/(\pi R)$

θ : Blade pitch angle,deg

$\theta(\psi)=\theta_0+\theta_{1C}\cos(\psi)+\theta_{1S}\sin(\psi)$

1 INTRODUCTION

For more than twenty years, ONERA has been conducting rotor tests in the S1.MA wind tunnel to supply AEROSPATIALE Helicopters Division with the information required to develop its helicopters. During this period, there have been major changes in the test facilities and objectives.

The original test rig used no longer allowed tests to be conducted with the required productivity. A new test rig was therefore designed and built. The qualification test took place in November 1987.

The first test, requested jointly by AEROSPATIALE Helicopters Division and ONERA Aerodynamic Department, took place in August1988. The tests concerned comparison of five rotors which differed only by their blade tips. To highlight the gains and performance of one rotor with respect to the other, it was necessary to completely change the test procedure.

The purpose of this document is to describe the new rotor test rig now operational in the S1.MA wind tunnel of the Modane-Avrieux Center and the new method used to compare rotors as well as the quality of the results obtained.

2 THE NEW TEST RIG

This section is a brief history recalling the reasons which led to the design of a new test rig, the design specifications and finally the description of the rig.

2.1 Historical Review

The first rotor test rig used in the S1.MA wind tunnel (Fig. 1) allowed a large number of test campaigns to be carried out (Ref. [1], [2], [3], [4]).

Nine of these campaigns were conducted for the AEROSPATIALE Helicopters Division. During these nine campaigns, the test objectives considerably changed. As the models progressed in the direction of an increasingly faithful representation of the real rotors, the test objectives evolved from basic research to gain a better understanding of operation of rotors and define the extreme limits of their domain of use to measurements disigned to guide industrial choices. Considering these la objectives, the old test rig had two major shortcomings :

-Subsequent to a ground resonance which was observed during the eighth campaign, a strut was added to rigidify the structure supporting the rotor shaft. This strut then made it impossible to tilt the rotor shaft during rotation. The result was an increase in the test time and a limitation in exploration of the flight envelope.

-The second problem of this test rig was the prohibitive installation time, since it was necessary to first install the drive system located in the test section downstream of the rig, then to install the rig itself, make the alignments which were difficult operations and finally install the rotor. One of the wind tunnel chariots (movable test sectior

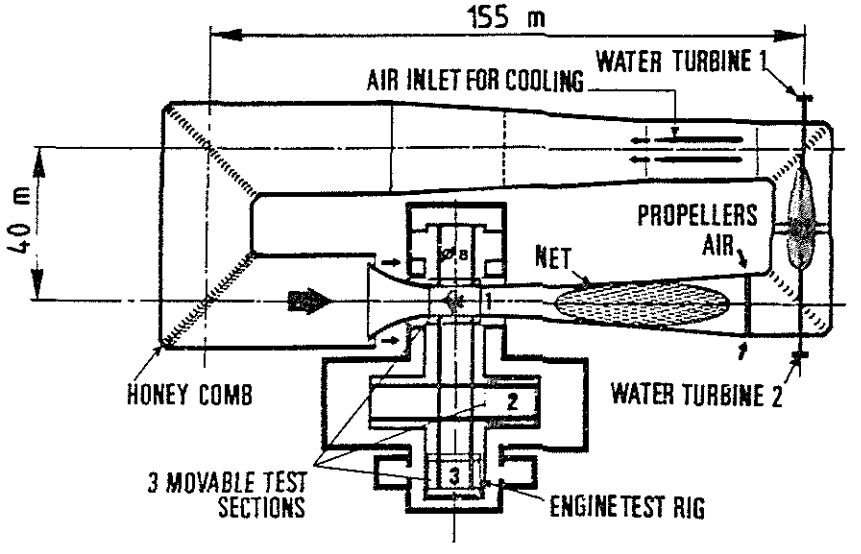

Fig. 1 -S1.MA large atmospheric wind tunnel schematic

was immobilized for one month to prepare the test.

These shortcomings led ONERA to design a new test rig in order to increase the productivity and decrease the cost of the rotor tests and improve the quality of measurements.

Initial work was started on this new test rig in 1982, funded jointly by ONERA and the Direction Générale de l'Aviation Civile (French counterpart of the FAA). Site acceptance took place in 1985 and the qualification test in November 1987.

2.2 Specifications of the New Rotor Test Rig

This test rig is designed to be installed in the large S1.MA wind tunnel of the Modane-Avrieux Center. The test section is 8 meters in diameter and 14 meters in length. For helicopter rotor test the maximum airspeed used is 130 m/s but this wind tunnel is able to reach M = 1.

The main specifications of the new rig are very similar to those of the original rig. Only certain technical solutions are different.

- The new rig is capable of driving helicopter or tilt rotor aircraft rotors up to 5 meters in diameter. In order to be able to test a 5 meters tilt rotor, power and drive torque characteristics are imposed as well as the rotor tilt angle. These characteristics are as follows :
  - maximum power 500 kW
  - maximum torque 7000 Nm at 680 rpm
  - tilt angle between +25 degrees and -95 degrees with a positioning accuracy of ±0.02 degrees.
- The rotation speed range varies from 0 to 1100 rpm. As regards test rig and model safety, control of the rotation speed is an essential factor in definition of the rig. In addition to the speed range, other constraints had to be taken into account, i.e. :
  - the rotor must never be stopped in presence of wind in the test section
  - the rotor must not be subjected to fast variations in rotation speed.
- These constraints require very sophisticated regulation whose main function is to insure the stability of the rotation speed. During the phases of variation of a parameter, the stability is insured within ±2 percent. During the so called "stabilized" measurement phase, the speed must be held within ±0.2 percent.
- Both directions of rotation must be possible.
- An important specification concerns the rigidity of the test rig. The frequency of the first longitudinal eigenmode must be higher than the rotation frequency so as to avoid any risk of ground resonance.
- The test rig installation and removal times must be as short as possible in order to improve the productivity of the test. The target set for installation of the test rig is to immobilize the chariot for only four days before entry in the aerodynamic circuit.
- Finally, the quality of all the measurements must be such as to achieve an overall accuracy of rotor performance measurements of approximately ±1 percent.

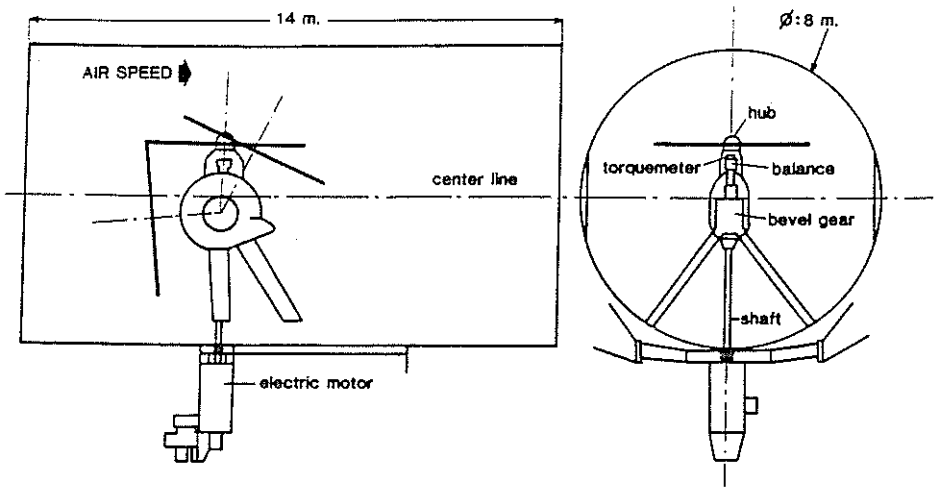

Fig. 2 -New rotor test rig

2.3 - Description of the Rotor Test Rig

The test rig includes three main parts (Fig. 2) :

- the drive system,
- the structure supporting the rotor,
- the measuring instruments.

2.3.1 Drive System

An electric motor drive system was selected for reasons of cost and ease of implementation. This solution, bulkier than a hydraulic solution, precludes installation of the motor directly at the end of the rotor drive shaft. It therefore requires a support with a tilting and driving system.

The drive motor is installed vertically under the test section, in the plenum chamber. It is a DC motor whose speed is controlled by modulating the current within the usual range (700 to 1100 rpm). To insure perfect speed control, this drive motor operates using several systems permanently installed in the basement of the wind tunnel. The systems mainly include the DC generator and backup systems in case of a line power failure (Fig. 3).

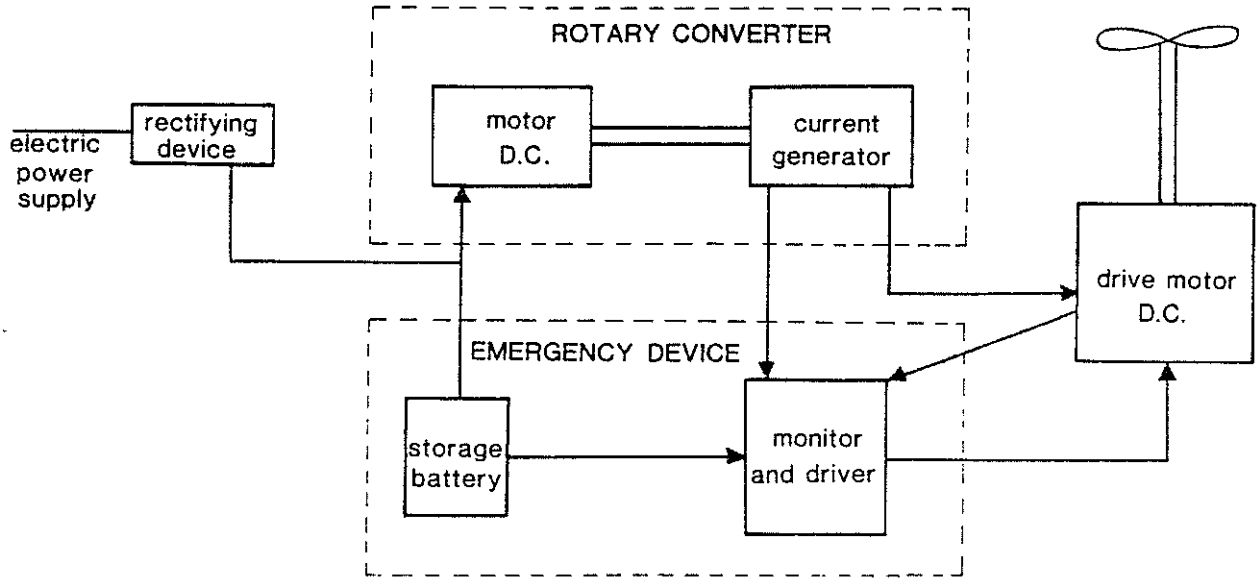

Fig. 3 -Motorization block diagram

A supervision system is provided to protect against the various cases of failure :

-short power cut, by the inertia of the DC generator

-power cut, by batteries for 2 minutes

-direct switchover to the batteries in case of a failure detected on the converter unit.

2.3.2 Supporting Structure

The structure supporting the rotor which tilts the rotor shaft and drives it in rotation, is called bevel gear. In order to be able to test tilt rotor craft with 5-meter diameter rotors, the tilting center must be located near the center line of the test section. This constraint is a drawback for rigidity, since it is necessary to locate the bevel gear, with many mechanical parts, relatively high in the test section (Fig. 4).

The solution adopted consisted in building a bevel gear, as light as possible, supported by four legged structure.

The streamlined beams forming this structure are made of steel. At the bottom, they are suported on very rigid consoles fixed on the chariot. The utilities required for the tests, hydraulic, pneumatic and electrical lines, go through the fairings.

The bevel gear includes a fixed part and a tilting part made of light alloy. Tilting is achieved by a motor-driven gear-wormscrew assembly. Another gear-wormscrew assembly insures locking in position. The automatic control system has a position and speed feedback loop. The maximum tilting rate is 2 deg/s.

2.3.3 Measuring Instruments

The measuring instruments are an integral part of the test rig, since they provide the mechanical linkage between the tilting part of the bevel gear and the rotor. In Figure 5 can be seen :

- the balance for weighing the aerodynamic loads,
- the torquemeter and flectors.

2.3.3.1 Balance

The balance is a nonrotating balance with assembled plates, connected by six dynamometers. The lower plate is attached to the tilting part of the bevel gear and the upper plate supports the rotor.

The dynamometers are interchangeable. In helicopter mode, three dynamometers measure the lift force, the roll and pitch moments, two measures the lateral force and rotor bearing friction moment and one measures the propulsive force. Their rigidity is a major factor in the overall rigidity of the test rig. They are therefore generally overdimensioned with respect to the loads developed by the rotor. In the current version, the balance has a drag dynamometer with a capacity of 10,000 N. All other dynamometers have a capacity of 20,000 N. To insure good sensitivity, the dynamometer part is designed so that the useful operating range corresponds to the dynamic range of the S1.MA wind tunnel measurement system.

This overcapacity is an advantage and a safety factor for such tests, where dynamic excitation can overcomes the average values of the loads to be measured. The balance is also equipped with a safety device which can lock the upper plate. Three remote control locks are actuated if one of the dynamometers exceeds a preset load.

2.3.3.2 The Torquemeter and Flectors

The torquemeter is a thin tube used to measure the motor torque supplied to the rotor. It is located on the transmission line inside the balance. It has a capacity of 3000 Nm for helicopter tests.

The flectors, which are elastic decoupling devices, are located on either side of the torquemeter. They insure the transmission of the motor torque while being axially very flexible so as not to short circuit the balance. A strain gage bonded to the upper flector allows the residual stiffness of this element to be taken into account.

These strain gages are located on the rotating part. To transmit their signals, a slipring is located inside the transmission shaft. This slipring, which does not transmit the rotor torque, transmits all the inputs from the rotor hub. It includes 137 measurement tracks and 13 power tracks.

2.3.4 Acquisition System

The S1.MA acquisition system is equipped with 80 analog channels. All the signals are filtered by low-pass filters (KEMO - 24 dB/octave) set at different frequencies according to the type of acquisition :

Global weighings (filters set at 0.5 Hz) : when the rotor balance conditions are achieved, the signals are digitized ten times at a rate of one acquisition per second. The average of these signals is used to compute the performance.

Harmonic analysis (filters set at 200 Hz) : after a global weighing, all the signals relative to the dynamic measurements, generally blade bridges, are digitized on 64 points per revolution for ten consecutive revolutions.

2.3.5 Use of the New Test Rig

With this new test rig, preparation of a test begins directly with installation of the rotor. In effect, the storage platform and handling facilities are disigned to carry out this operation without having to immobilize a chariot. Light-weight platforms allow work to be done on the rotor under good conditions.

When this first operation is completed, the entire supporting structure is transported in the chariot (Fig. 6). No mechanical adjustments are required as the position of the test rig on its anchor points was marked during acceptance operations. All the mechanical, hydraulic, pneumatic and electrical interfaces are designed to be connected rapidly.

In the test section, work on the rotor is facilitated by the use of platforms which are rapidly in-

Fig. 4 - New test rig in S1.MA

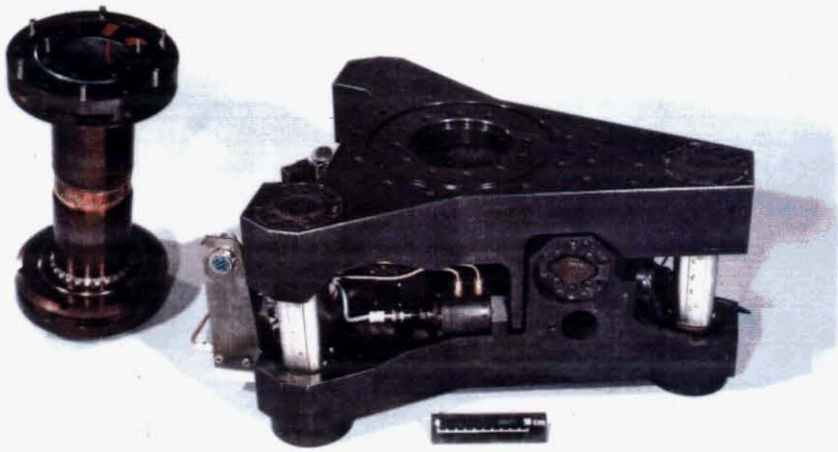

Fig. 5 - Torquemeter and 6 component-balance

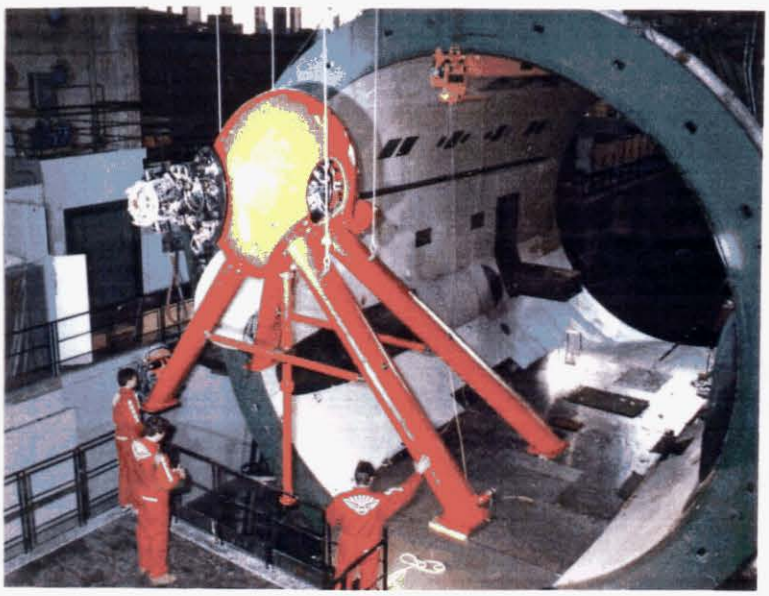

Fig. 6 - Getting into the test section

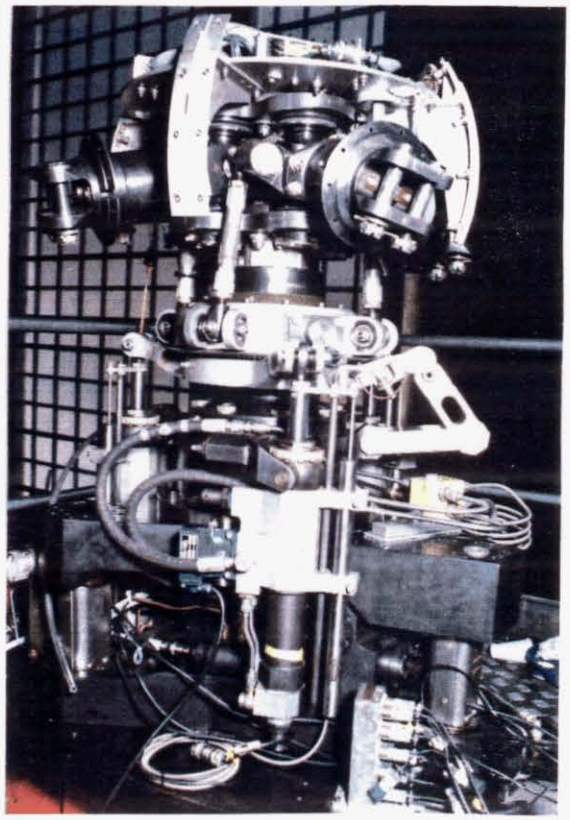

Fig. 7 - Hub mounted on rig

stalled and removed.

To control the rotor speed, it is sufficient to set the value to be reached and confirm this setting. The automatic control system then varies the speed to reach the required value complying with the speed and acceleration settings made. When the desired speed is achieved, the automatic controller performs regulation. This procedure substantially improves the productivity of this test rig by comparison with the old test rig on which the control was manual.

Tilting of the mast is controlled by the same principle or directly by pulses until the desired value is reached.

All these improvements were evaluated during the tenth rotor test campaign. They allowed use of a more efficient test method to compare rotors. This method is described in the next section.

3 WIND TUNNEL TESTS

3.1 Rotor Description

The rotors used during the tenth campaign are similar to those of a 1:4 scale SUPER PUMA. Model rotor blades are Mach scale.

3.1.1 Hub Description

Figure 7 is a photograph of the hub installed on the balance and the bevel gear. It is a four-blade articulated hub : the lead-lag and flapping hinges are at the same location .075 m from the rotor hub center, i.e. an off-centering of 3.5 percent. The pitch hinge is located beyond these hinges.

Angular frequency adaptors are installed on the lead-lag hinge and are used to handle any ground resonance problems : the first drag mode was thus increased from 0.26 Ω to 0.40 Ω.

The pitch control system consists of a fixed swash plate/rotary swash plate assembly driven by hydraulic actuators located at 120 degrees.

3.1.2 Description of the Blades

The technology used to produce the blades is very close to that used for full scale composite rotor blades. The spar is made of glass-fiber rovings and the rear part is filled with honeycomb.

The skin of the blade consists of layers of carbon fiber at 45 degrees whose thickness decreases towards the trailing edge. Chordwise balancing is achieved through adding INERMET counterweight enbedded into the spar.

From a strictly dynamic point of view, the blades of this model are not identical to those encountered on a full scale rotor : the first flapping and drag modes are positioned as on a full scale four-blade rotor, but the frequency of the first torsion mode is higher than that encountered on most AEROSPATIALE helicopters.

The rotors tested during the tenth campaign included two families of blades. The basic rotor blade had a rectangular tip. The others had an SPP8 tip (Fig. 8) with different anhedral definitions, one of these is identical with the new main rotor of the SUPER-PUMA MK2.

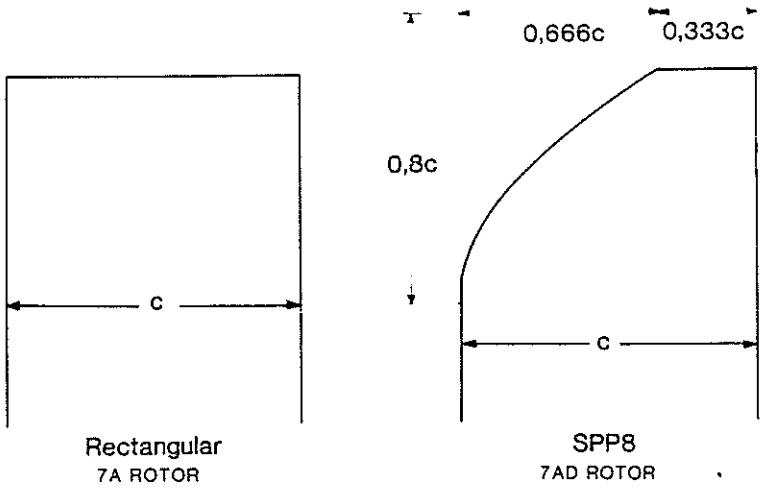

Fig. 8 -Blade tip shapes

The main characteristics of these two sets of blades are as follows :

	7A MODEL	7AD MODEL
Basic chord (m)	0.14	0.14
Radius (m)	2.1	2.1
Number of blades	4	4
Solidity	0.085	0.085
Cutout (r/R)	0.202	0.202
Airfoils :		
0.202 R to 0.75 R	0A213	0A213
0.9 R to R	0A209	0A209
Hub offset (m)	0.075	0.075
Tip shape : (figure 8)	Rect.	SPP8

3.1.3 Description of the Instrumentation

Figure 9 shows the radial distribution of the strain gages that measure the bending and torsion moments along the blade. Two pitch control rods and the rotation scissors are also equipped. The mast also includes gages to measure its bending. Flapping and lead lag angles are measured on the hinge of one blade, pitch angle is measured on the hinge of each blade. All these measurements are made in a rotating reference frame and are transmitted to the acquisition system through the slip-ring. The displacement of the control actuator rods is also measured, in a fixed reference frame.

The performance of the different rotors is evaluated from the direct measurements made by the balance and the torquemeter.

During the tenth test campaign, noise measurements were also made using eight microphones located around the rotor. These measurements, made in the guided test section without acoustic treatment on the wind tunnel walls, were sensitive to the many reflections on the walls. For the next test campaign, it was decided to cover the walls with an absorbent coating in order to decrease these reflection phenomena to a minimum.

3.2 Test Program

The purpose of the tenth rotor test campaign at Modane-Avrieux, was to compare the performance, vibration and noise of the rotors with different blade tips.

Earlier (Ref. [5]), the tests were conducted at iso-α_s. A collective pitch scan was made for various advance parameters. The influence of compressibility was studied at constant advance ratio, conducting the test at different rotor speeds. To compare the rotor performance, it was then necessary to smooth the performance measurements to arrive at constant speed, lift, propulsive force and peripheral Mach number. The smoothing method used is described in document Ref. [5]. As for all smoothing methods, small uncertainties appear at the limits of the test domain and detailed rotor comparisons may then be biased. In addition, the comparison of the loads and vibrations was very difficult.

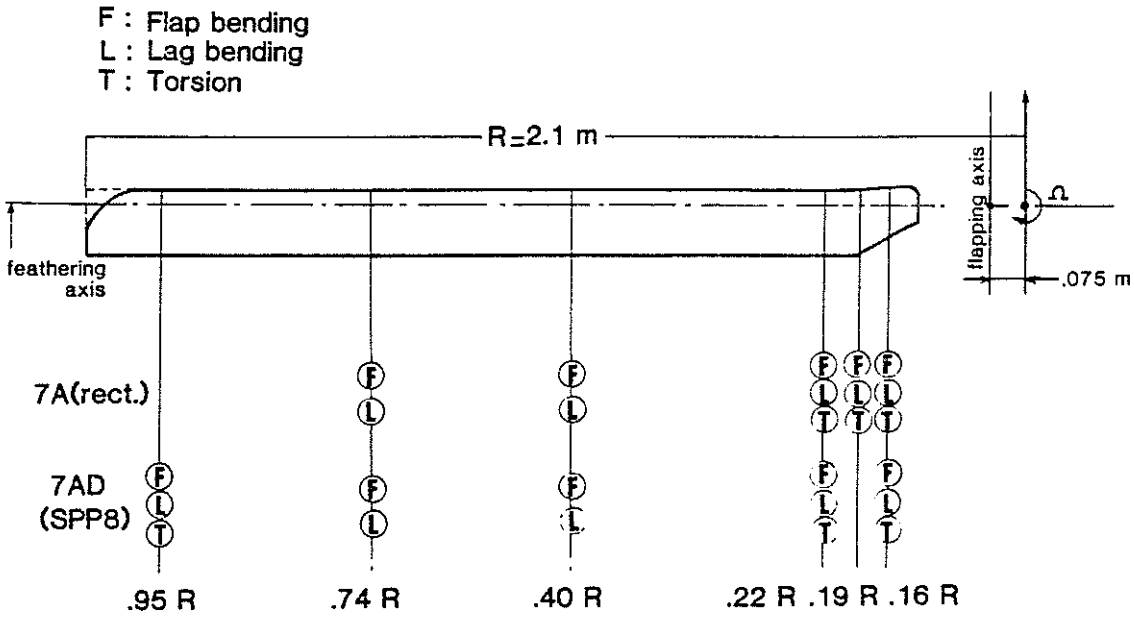

Fig. 9 - Blade instrumentation

To overcome these difficulties, it was decided to conduct the tests under the following imposed conditions :

Lift coefficient : $C\ell/\sigma$

Propulsive coefficient : $\overline{X}$

Tip Mach number : Mtip

Advance ratio : μ

Figure 10 shows the parameters scanned during the tenth campaign : the test range in lift and speed is very large.

On a helicopter, in flight, the roll and pitch moments generated on the rotor by the longitudinal and lateral cyclic pitch controls balance the roll and pitch moments generated by the aerodynamic forces applied to the airframe. This balance does not exist in the wind tunnel and it is therefore necessary to impose two additional conditions for cyclic control of the rotor. Generally in the wind tunnel, the lateral and longitudinal cyclic pitches are adjusted so that the first harmonic of the flapping angle is zero (Ref. [6], [7], [8], [9], [10]). In Modane-Avrieux, the cyclic control law is chosen such that :

longitudinal cyclic pitch = longitudinal tilt
$(\theta_{1s} = \beta_{1c})$

lateral tilt=0 deg $(\beta_{1s} = 0$ deg$)$

This control law has the advantage of being the best tradeoff of control loading and bending moments along the blade, as is shown by figure 11, allowing the test domain to be as large as possible. During the campaign specific tests showing the influence of the control laws were run.

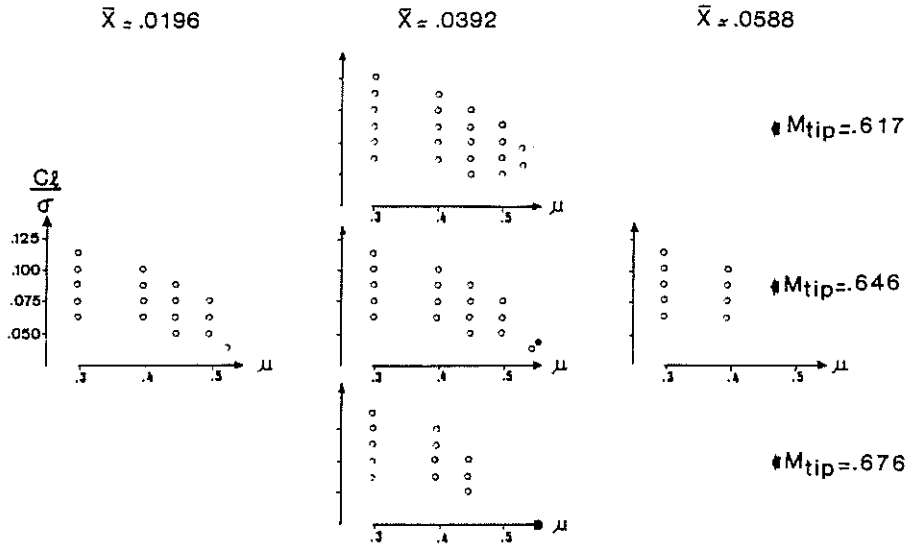

Fig. 10 - Test range

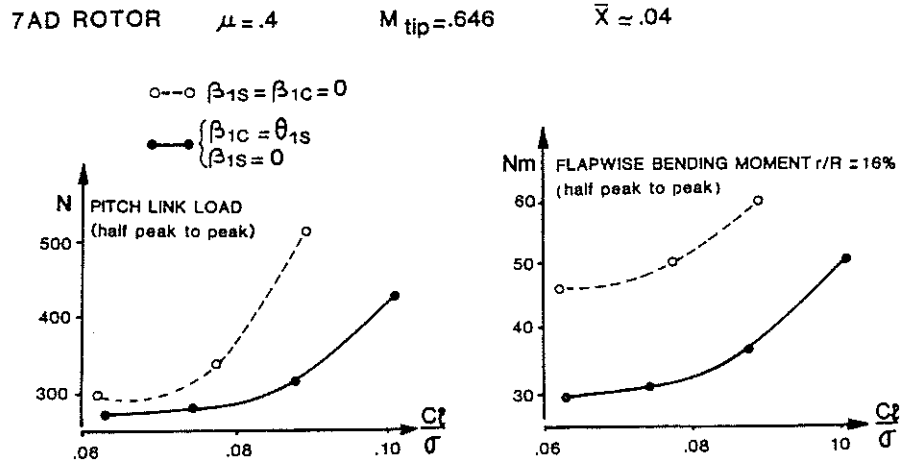

Fig. 11 - Cyclic laws influence on rotor dynamic loads

3.3 Description of the Control Aid Program

In order to facilitate rotor comparisons, as was seen above, it is preferable to impose loads. The cyclic control law also requires imposing additional constraints between the single cycle flapping and pitch movements.

The point where the measurements are made is therefore reached after several iterations on the following rotor control parameters :

Collective pitch (θ_0)

Lateral cyclic pitch (θ_{1C})

Longitudinal cyclic pitch (θ_{1S})

Mast tilt angle (α_S)

If these iterations are made by trial and error, it is very long and difficult to obtain a point. To overcome this problem, an automatic control aid system was developed. Its operating principle, based on an iterative process, is as follows :

0 - Choice of the test configuration $(C_\ell/\sigma)^0, \overline{X}^0, \mu, M_{tip}$ with the chosen control law

1 - Initialization of $\theta_0, \theta_{1C}, \theta_{1S}, \alpha_S$ from earlier tests or prior theoretical computations

2 - Measurements of $C\ell/\sigma, \overline{X}, \beta_{1C}, \beta_{1S}$ due to these commands

3 - Search for the matrix of partial derivatives to determine the Jacobian [J]

$$[J]=\begin{bmatrix} \frac{\partial(C_\ell/\sigma)}{\partial\theta_0} & \frac{\partial(C_\ell/\sigma)}{\partial\theta_{1C}} & \frac{\partial(C_\ell/\sigma)}{\partial\theta_{1S}} & \frac{\partial(C_\ell/\sigma)}{\partial\alpha_S} \\ \frac{\partial\overline{X}}{\partial\theta_0} & \frac{\partial\overline{X}}{\partial\theta_{1C}} & \frac{\partial\overline{X}}{\partial\theta_{1S}} & \frac{\partial\overline{X}}{\partial\alpha_S} \\ \frac{\partial(\theta_{1S}-\beta_{1C})}{\partial\theta_0} & \frac{\partial(\theta_{1S}-\beta_{1C})}{\partial\theta_{1C}} & \frac{\partial(\theta_{1S}-\beta_{1C})}{\partial\theta_{1S}} & \frac{\partial(\theta_{1S}-\beta_{1C})}{\partial\alpha_S} \\ \frac{\partial\beta_{1S}}{\partial\theta_0} & \frac{\partial\beta_{1S}}{\partial\theta_{1C}} & \frac{\partial\beta_{1S}}{\partial\theta_{1S}} & \frac{\partial\beta_{1S}}{\partial\alpha_S} \end{bmatrix}$$

These partial derivatives are evaluated by successive increments on the various commands by finite differences. For instance :

$$\frac{\partial\beta_{1S}}{\partial\theta_0}=\frac{\beta_{1S}(\theta_0+\Delta\theta_0)-\beta_{1S}(\theta_0)}{\Delta\theta_0}$$

This complete evaluation of the Jacobian therefore requires four increments on each of the commands which are applied by the pilot and four measurements of the equilibrium parameters.

4 - Computation of the new command

$$[X]_i = [\theta_0, \theta_{1C}, \theta_{1S}, \alpha_S]_i$$

from the Newton-Raphson recurrence formula

$$[X]_{i+1} = [X]_i - [J]^{-1}\,[Y]_i$$

where:

$$[Y]_i = [C\ell/\sigma - (C\ell/\sigma)^0, \overline{X} - \overline{X}^0, \theta_{1S} - \beta_{1C}, \beta_{1S}]_i$$

5 - Application of the new commands by the pilot

6 - Measurement of the new $C\ell/\sigma, \overline{X}, \beta_{1C}, \beta_{1S}$

7 - Operations 4 for to 6 are repeated until $[Y] = [0]$

This process is similar to the one adopted in the rotor computation models. The only difference consists of replacing the theoritical rotor model by the direct measurements made on the rotor in the wind tunnel.

This automatic system, programmed on the central computer of the wind tunnel which also manages acquisition and supervision of the test, guides the pilot by suggesting values of the commands to be applied to the rotor. These values appear on a screen located in the test control room.

This program has the advantage of helping in rotor control and improving the accuracy in obtaining the lift and propulsive force objectives, which then facilitates comparison of the rotors.

3.4 Test Methodology

The test method consists of consecutively "weighing" the various sets of blades mounted on the same hub and comparing their performance computed from the filtered signals.

The hub effect is not negligible (fig. 12). The tests begin by weighing the hub without rotating blades for several advance ratio, rotor shaft angles and collective pitches. The global weighing is then corrected for hub effects to obtain the performance of the set of blades.

drifts in the measurement apparatus. The reproducibility of the tests is satisfactory. For rotor 7A (Fig. 13), the differences on the pitch settings are less than ±0.05 degrees. Under these conditions, the accuracies observed on the main parameters are :

motor torque : $\Delta C_Q/C_Q = \pm .7\ \%$

lift : $\Delta C_\ell/C_\ell = \pm .8\ \%$

propulsive force : $\Delta C_D/C_D = \pm 2.7\ \%$

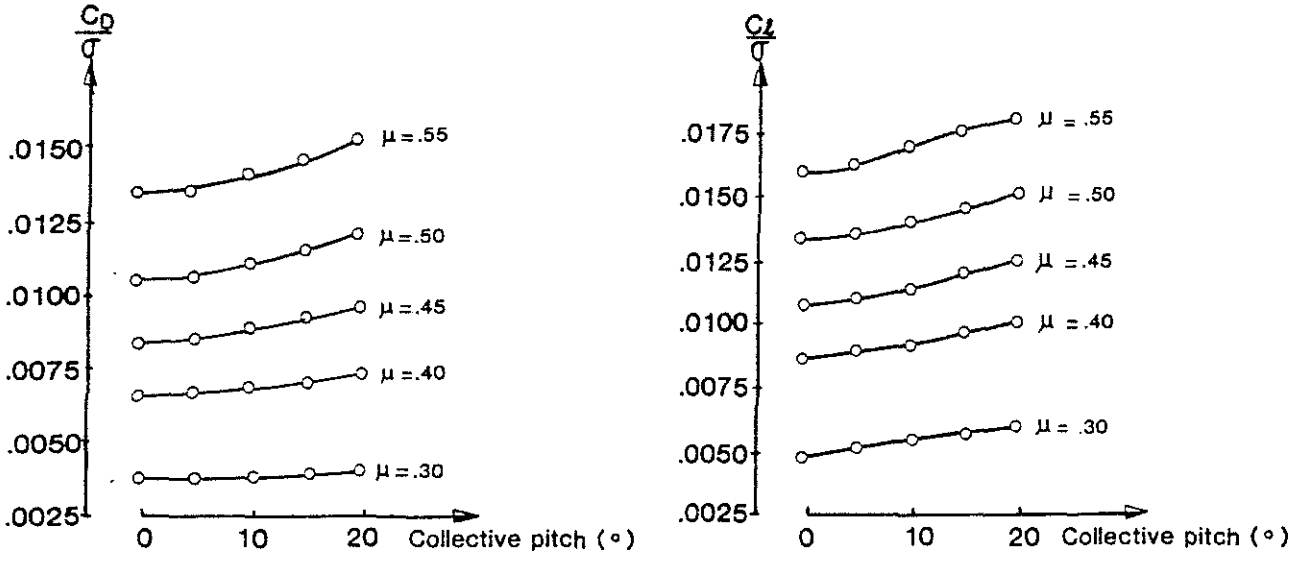

Fig. - 12 Blade-off performance

3.5 - Quality of the Measurements

The results given in this section are aimed at demonstrating the quality of the measurements obtained with the new test rig. This quality is highlighted from the repeatability tests, the performance between rotors and the various local values measured on the rotor.

3.5.1 Repeatability tests

During the tests, repeatability tests were conducted in order to make sure there were no

The inaccuracy on the propulsive force in the aerodynamic axes is due to the uncertainty on the balance (±5 N) and the projection of the lift uncertainty (±30 N) on the propulsive force axis.

For a propulsive force coefficient set under these conditions, the curve of lift versus torque is

supplied in the test domain with an accuracy of around 1 percent, which is the stated goal.

3.5.2 Performance Measurements - Rotor comparison

Figure 14 shows the comparative performance of the basic 7A rotor and the 7AD rotor with SPP8 tips whose anhedral is identical to that of the new SUPER-PUMA MK2 main rotor. The comparisons are established for advance ratio $\mu = 0.3$, 0.4, 0.45 and 0.5 for a propulsive force coefficient $\bar{X} = 0.04$. The gains in performance of rotor 7AD are approximately 3 to 5 percent for low lifts. For higher lifts, at $\mu = 0.3$ and 0.4, the two rotors are equivalent, whereas for $\mu = 0.45$ and $\mu = 0.5$, rotor 7AD is always more performing.

3.5.3 Measurement of Loads on the Rotor

The curves given in this section show typical examples of comparisons now made possible by the control method. In fact, this new procedure allows load comparisons to be made directly on a rotor by varying a single parameter while maintaining all the other parameters constant. It obviously allows comparisons to be made between the different rotors as well.

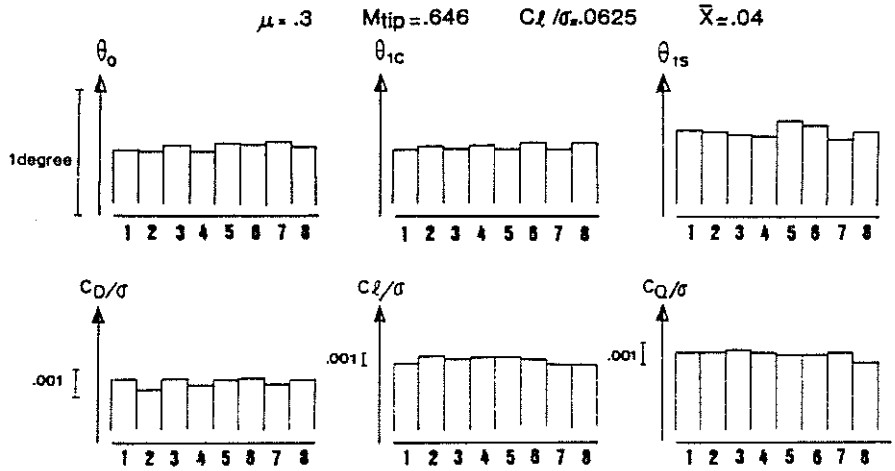

Fig. 13 - Comparison of test data repeatability

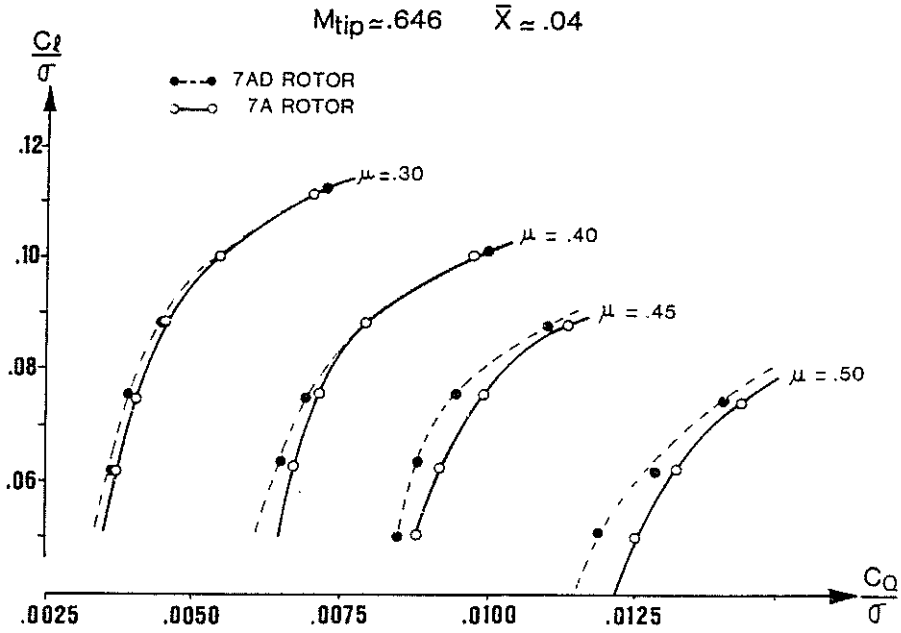

Fig. 14 - Rectangular tip - SPP8 tip performance

3.5.3.1 Control Loading

The influence of lift on the control loading can be observed in Figure 15 for $\mu = 0.3$, $M_{tip} = 0.646$ and $\overline{X} = 0.04$. When the lift increases, large oscillations appear on the retreating blade. They can be explained by a stall on the retreating blade with excitation of the blade torsion mode.

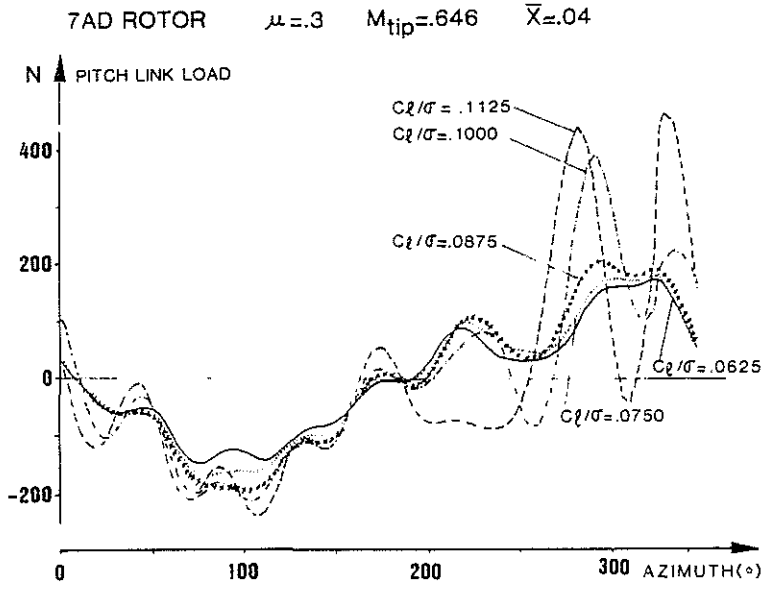

Fig. 15 - Rotor lift influence on pitch link load

Figure 16 shows the influence of the advance ratio on the control loading for $C\ell/\sigma = 0.075$, $M_{tip} = 0.746$ and $\overline{X} = 0.04$.

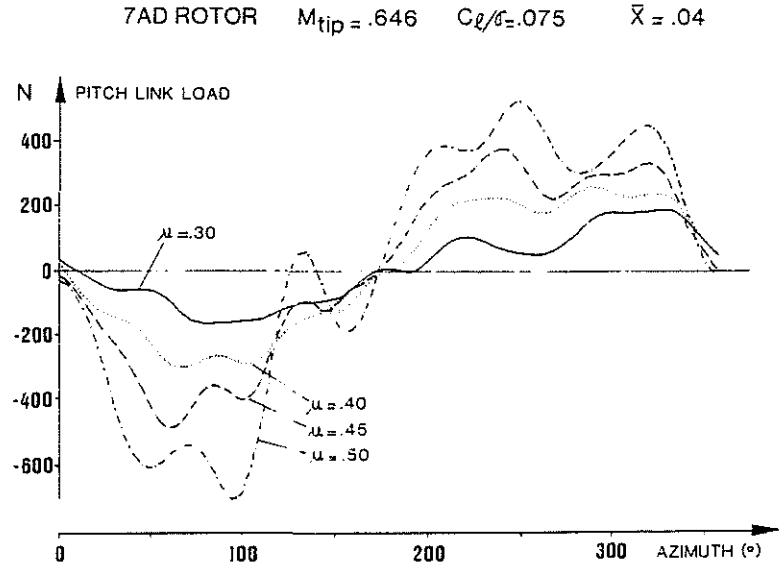

Fig. 16 -Advance ratio influence on pitch link load

3.5.3.2 Flapping and Edgewise Bending Along the Blade

Figure 17 shows the importance of lift on the amplitude of the edgewise bending moment for $\mu = 0.3$, Mtip = 0.646 and $\overline{X} = 0.04$.

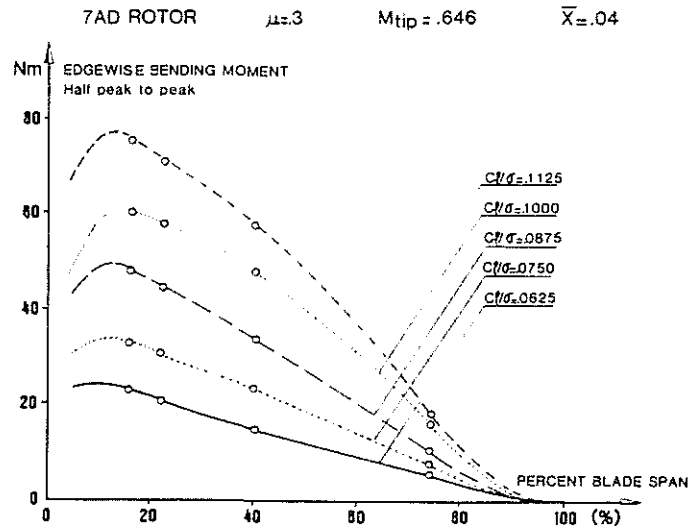

Fig. 17 - Rotor lift influence on edgewise bending moment

Figure 18 shows the influence of the advance ratio on the amplitude of the flapping moments for $C\ell/\sigma = 0.75$, $M_{tip} = 0.746$ and $\overline{X} = 0.04$.

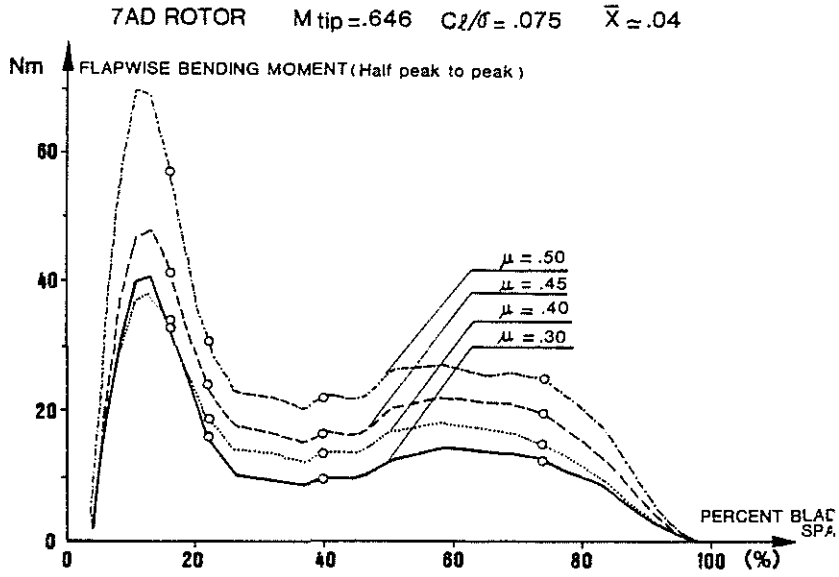

Fig. 18 -Advance ratio influence on flapwise bending moment

4 CONCLUSION

The new helicopter rotor test rig of the S1.MA wind tunnel (ONERA - Modane-Avrieux Center) allowed the tenth test campaign to be conducted in August 1988 for AEROSPATIALE Helicopters Division and ONERA Aerodynamic Department.

This campaign first showed that this new test rig amply covered the flight envelope of current helicopters both for lift and speed. Realistic flight cases were even simulated at very high speeds (V = 400 km/h). It also demonstrated that the goal of increasing the productivity was achieved, since five rotors were tested and compared in three weeks.

This test rig also allowed use of a new test method for comparing rotors at constant lift and propulsive force, thereby facilitating analysis of the results from the standpoint of performance and also of load and vibration.

New uses are planned in the near future for this test rig. At the beginning of 1990, a typical helicopter test will take place with highly instrumented blades (strain gages and pressure transducers) and also with the presence of a fuselage under the rotor. This campaign will be followed by the test on the EUROFAR European tilt-rotorcraft rotor model.

5 REFERENCES

[1] M. Lecarme, Comportement d'un rotor au-delà du domaine de vol usuel à la grande soufflerie de Modane.
AGARD Fluid Dynamics Panel Specialists' Meeting, Sept. 1972

[2] A. Bremond, et al. Design and Wind Tunnel testing of 1.5 M Diameter Model Rotors,
4th European Rotorcraft Forum - Sept. 1976

[3] J.P. Silvani, et al., Aerospatiale Survey of Wind Tunnel testing of Smal and Large Scale Rotors,
7th European Rotorcraft Forum - Sept. 1981

[4] G. Leclère, et al. Moyens d'essais d'hélice et de rotors de l'ONERA
19e Colloque d'Aérodynamique Appliquée de l'AAAF, Nov. 82

[5] J.P. Drevet et al., Essais Comparés de Rotor d'Hélicoptère en Soufflerie,
19e Colloque d'Aérodynamique Appliquée de l'AAAF, Nov. 82

[6] M. Stephan et al., A New Wind Tunnel Test Rig for Helicopter Testing,
14th European Rotorcraft Forum - Sept. 1988

[7] H.L. Kelley et al., Aerodynamic Performance of a 27 Percent-Scale AH-64 Wind Tunnel Model with Baseline/Advanced Rotor Blades,
41st American Helicopter Society Annual Forum, May 1985

[8] J. Cowan et al., Wind Tunnel Test of a Pressure Instrumented Model Scale Advance rotor
42st American Helicopter Society Annual Forum, June 1986

[9] L. Dadone et al., Model 360 Rotor Test at DNW - Review of performance and Blade Airload Data,
AGARD Fluid Dynamics Panel Specialists' Meeting, Sept. 1972

[10] W.T. Yeager et al., Wind Tunnel Evaluation of an Advanced Main Rotor Blade Design for a Utility Class Helicopter,
NASA TM 89129, Sept. 87

[11] M. Torres et al., Improving Helicopter Aerodynamics - A Step Ahead,
14th European Rotorcraft Forum - Sept. 1988